

Dependencies of secondary electron yields on work function for metals by electron and ion bombardment

M. Kudo, Y. Sakai, and T. Ichinokawa

Citation: *Appl. Phys. Lett.* **76**, 3475 (2000); doi: 10.1063/1.126682

View online: <http://dx.doi.org/10.1063/1.126682>

View Table of Contents: <http://apl.aip.org/resource/1/APPLAB/v76/i23>

Published by the [American Institute of Physics](#).

Additional information on *Appl. Phys. Lett.*

Journal Homepage: <http://apl.aip.org/>

Journal Information: http://apl.aip.org/about/about_the_journal

Top downloads: http://apl.aip.org/features/most_downloaded

Information for Authors: <http://apl.aip.org/authors>

ADVERTISEMENT



Goodfellow
metals • ceramics • polymers • composites
70,000 products
450 different materials
small quantities fast

www.goodfellowusa.com

Dependencies of secondary electron yields on work function for metals by electron and ion bombardment

M. Kudo and Y. Sakai

JEOL Ltd. 3-1-2 Musashino, Akishima, Tokyo, 196-8558 Japan

T. Ichinokawa^{a)}

Department of Applied Physics, Waseda University, 3-4-1, Okubo, Shinjuku-ku, Tokyo, 169-8555 Japan

(Received 27 September 1999; accepted for publication 11 April 2000)

Secondary electron yields depending on work function were measured for 30 species of metal in ultrahigh vacuum by electron and ion bombardment. Secondary electron yields induced by electrons at 10 keV increase with work function, while those by Ar⁺ ions at 3 keV decrease with increasing work function. The opposite dependencies of secondary electron yields on work function between electron and ion bombardment are discussed on the basis of the different mechanisms of secondary electron emission, i.e., kinetic and potential emission for electron and ion bombardment, respectively. © 2000 American Institute of Physics. [S0003-6951(00)01023-8]

It is well known that the contrast of the secondary electron image of scanning electron microscopy (SEM) is different from that of scanning ion microscopy (SIM). For example, we reported¹ that the atomic number (Z) dependence of the image contrast in SEM for several metals (Al, Cu, Ag, and Au) is opposite to that in SIM observed by focused Ar⁺ or Ga⁺ ion beam. This fact was explained by the different parameters of the primary beams, namely, the backscattered electrons depending on Z contribute to secondary electron emission for electron bombardment, while the backscattering ions depending on Z become lost for ion bombardment. These behaviors are caused by different ranges between electrons and ions.

Secondary electron emission induced by electrons²⁻⁶ and ions⁶⁻⁸ has been reported in a number of articles, however, the dependency of secondary electron yields on material parameters has not been completely clarified.

In this letter, the secondary electron yield δ and the work function Φ were directly measured for 30 species of metals in ultrahigh vacuum from integrated intensities and onset energies of secondary electron spectra emitted by electron and ion impact. The results show that the dependencies of δ on Φ are opposite between electron and ion impact. This fact is very important for the analysis of the material by SEM and SIM. Furthermore, discussions on these phenomena are important for understanding the mechanisms of secondary electron emission for electron and ion bombardment.

The experimental apparatus used in this experiment is a scanning Auger electron microscope (JAMP-7800F) with a vacuum pressure of 5×10^{-8} Pa, which is equipped with a hemispherical electron energy analyzer, an electron optical column, and an Ar⁺-ion sputtering gun. The energies of electron and Ar⁺-ion beams were 10 and 3 keV, and the incident angles were 35° and 50° from the specimen surface for electron and ion bombardment with analyzing the kinetic energy of secondary electrons emitting in the direction normal to the surface. The specimens are polycrystal pure metals of 30

species (UHV-EL-3700) prepared by Geller Analytical Laboratory, and the surfaces of those metals are cleaned by Ar⁺-ion sputtering in ultrahigh vacuum. The secondary electron spectra were measured by the hemispherical electron energy analyzer using an operation mode of constant potential ratio (the ratio between pass energy in the spectrometer and kinetic energy of measuring electrons is a constant) at 0.22, and 0.05 eV steps for energy sweep with a dwell time of 20 ms at each step. In this mode, the relative energy resolution $\Delta E/E$ is a constant. The secondary electron yields were measured from the integrated intensities of secondary electron spectra in a range from 0 to 30 eV and the work functions Φ were measured simultaneously from the onset energies of secondary electron spectra by applying bias potential -5 V to the specimen. If the work function of tungsten, Φ_W , is put to 4.55 eV from the table in Ref. 9, the work functions of other metals are obtained simultaneously with δ by the measurement of secondary electron spectra.

Figures 1(a) and 1(b) show the secondary electron spectra induced by 10 keV electrons and 3 keV Ar⁺ ions for several metals with applying the bias potential -5 V to the specimen. The work functions Φ measured from an extrapolated or an inflected point of the initial rise of secondary electron emission have an accuracy of 0.05 eV. Here, we should notice that the widths of secondary electron spectra obtained by ion bombardment are narrower than those by electrons, and the widths by electrons are 25–30 eV, whereas those by ions are 10 eV. We should emphasize that the order of the magnitude of the integrated intensities among these metals is opposite between electron and ion impact, while the work functions measured for respective specimens by electron and ion impact are the same within an error of 0.05 eV.

In Fig. 2(a), open circles show the dependency of Φ on Z for 30 metals obtained by the present experiment and the values almost agree with those of the table in Ref. 9 shown by small dots. Figure 2(b) shows a relationship between δ and Z for electron bombardment. From Fig. 2(b), we can see that δ tends to increase with Z and has a similar periodicity to that of Φ . The maximum of δ in each period corresponds

^{a)}Electronic mail: ichinoka@jeol.co.jp

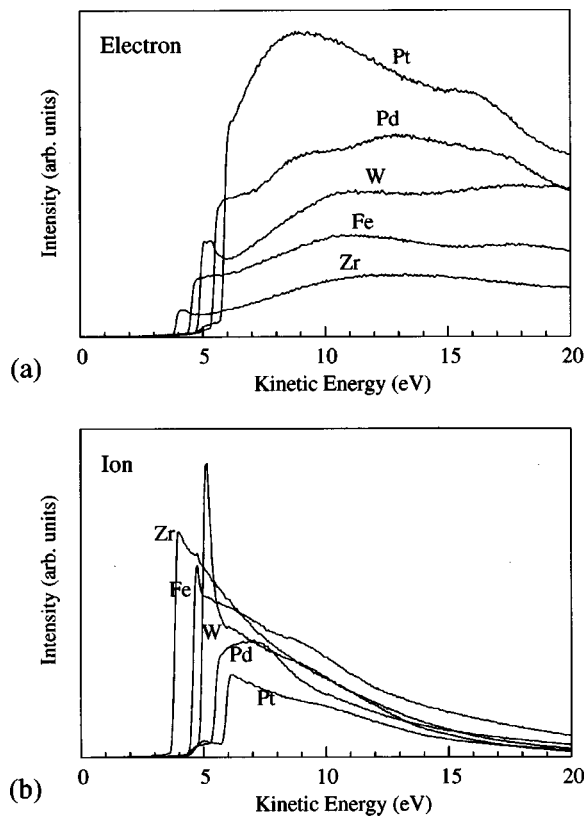


FIG. 1. (a) Secondary electron spectra induced by electrons at 10 keV and (b) Ar^+ ions at 3 keV for several metals. The bias potential of -5 V was applied to the specimen. The order of the magnitude of integrated intensities for the secondary electron spectra among the metals are opposite between electron and ion impact. On the other hand, the work functions measured from the onset energies of secondary electron spectra are the same between electron and ion impact for respective metals.

to that of Φ . On the other hand, Fig. 2(c) for Ar^+ -ion bombardment shows that δ tends to decrease with increasing Z and the maximum of Φ corresponds to the minimum of δ . Since the measured conditions for electron and ion impact are not the same, δ values are presented by arbitrary units in Figs. 2(b) and 2(c).

The dependence of δ on Z was already observed by Hippler, Hasselkamp, and Scharmann¹⁰ in the experiment of 100 keV H^+ , H_2^+ , and H_3^+ ion beams in ultrahigh vacuum for 27 metal species. The periodic behavior is similar to that of the present experiment shown in Fig. 2(b). This fact indicates that the mechanism of secondary electron emission produced by high-energy light ions is similar to that by electrons. In Fig. 2(b), δ increases with Z in each period and reaches the maximum at the boundary between the *A* and *B* groups in the periodic table, at which the *d*-shell electrons of the transition metals are completely filled. Beyond the maximum, δ decreases with increasing Z (electronegativity) in each period. Such a behavior of δ for electron bombardment is similar to that of Φ , while that for argon-ion bombardment is reverse, as shown in Fig. 2(c).

For the secondary electron emission by electron bombardment, we should consider several processes,¹¹ e.g., (1) production of internal secondaries in solid, (2) energy dissipation and cascade process of the incident electrons, (3) transport of excited secondaries from the bulk to the surface, and (4) escape process of secondary electrons across the sur-

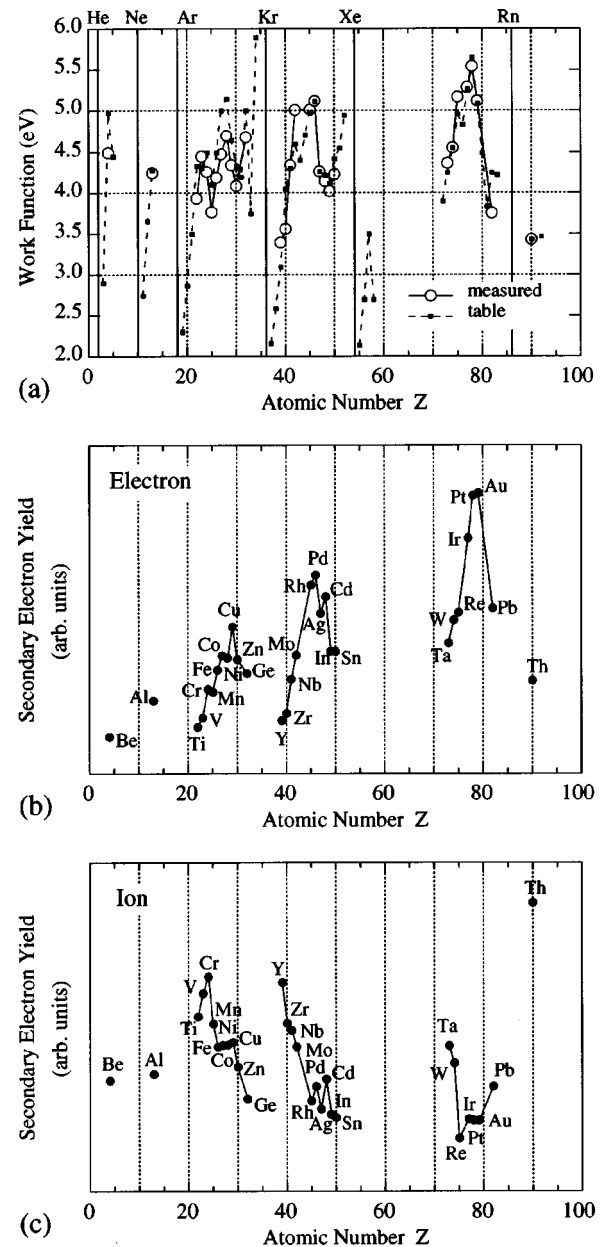


FIG. 2. (a) Work function Φ depending on atomic number Z , and (b) and (c) secondary electron yields δ depending on Z for electron and ion bombardment, respectively. The dependency of δ on Z for electron bombardment is similar to that of Φ , but that for Ar^+ -ion bombardment it is opposite to that of Φ .

face barrier. The dependence of δ on Φ was first discussed by Baroody¹² and Dekker.² However, a reliable analysis taking account of the above processes has been carried out by Schou.⁵ According to his equation, δ is influenced by the material parameters, the work function, and the electronic stopping power of the incident and emerging electrons. The production of the liberated electrons in solid depends on the local electron density (defined by the so-called local-density approximation¹³⁻¹⁵) through the stopping power. Since the work function is a measure of the energy difference between the Fermi level and the vacuum level, it is difficult to extract any general relationship between δ and Φ . However, the experimental data show that the dependence of δ on Z for electron impact has similar periodicity to that of Φ , and δ has a tendency to increase with Φ . This behavior cannot be exp-

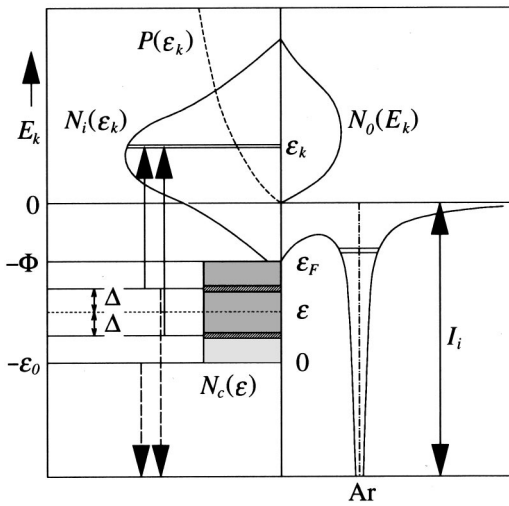


FIG. 3. Schematic diagram of the secondary electron emission caused by the direct Auger process of ion neutralization. $N_i(\epsilon_k)$ and $N_0(E_k)$ are energy distributions of liberated electrons in solid and emitted electrons into the vacuum, $P(\epsilon_k)$ is the escape probability across the surface barrier, $N_c(\epsilon)$ is the electronic density of states at the surface, and I_i is the ionization energy of Ar^+ ions.

lained by the analytical equation. One of the possibilities to explain this is the Monte Carlo simulation by using the loss function (dielectric function) as a material parameter.

In contrast, for low-energy heavy-ion impact, the velocity of Ar^+ ions at 3 keV (1.2×10^5 m/s) is much lower than those of electrons at 10 keV (6×10^7 m/s) and the Fermi electrons in metal (2×10^6 m/s). Therefore, the probability of kinetic emission is smaller than that of potential emission. The number of secondary electrons excited by ion neutralization, $N_i(\epsilon)$, was given by Hagstrum¹⁶ as a convolution of two densities of states at the surface, as shown in Fig. 3,

$$N_i(\epsilon) = \int_{-(\epsilon - \epsilon_F)}^{(\epsilon - \epsilon_F)} |\mu|^2 N_c(\epsilon + \Delta) N_c(\epsilon - \Delta) d\Delta, \quad (1)$$

where $|\mu|$ is a transition matrix of the Auger process and $N_c(\epsilon + \Delta)$ and $N_c(\epsilon - \Delta)$ are densities of states at energies of $\epsilon \pm \Delta$ for an initial state of the surface. The density of states at the surface $N_c(\epsilon)$ and the transition matrix $|\mu|$ are possible to put the constants for first approximation. This restriction means that $N_c(\epsilon)$ is independent of the bulk density of states of the conduction band. As shown in Fig. 3, since there are the following relationships between ϵ and ϵ_k , $\epsilon_k = I_i - \epsilon_0 + 2\epsilon$ and $\epsilon_0 = \epsilon_F + \Phi$ (where I_i is an ionization energy of Ar^+ ions), $N_i(\epsilon)$ is transformed to $N_i(\epsilon_k)$. With the escape probability $P(\epsilon_k)$, the intensity of emitted electrons into the vacuum, $N_0(\epsilon_k)$, is given as follows by using ϵ_k :

$$N_0(\epsilon_k) \propto P(\epsilon_k) N_i(\epsilon_k). \quad (2)$$

$P(\epsilon_k)$ was calculated by Hagstrum¹⁷ by taking into account the total refraction of secondary electrons at the surface:

$$P(\epsilon_k) = [1 - \{\Phi / (\epsilon_k - \epsilon_F)\}^{1/2}] / 2. \quad (3)$$

If E_k is set equal to the energy of escaped electrons into the vacuum, $E_k = \epsilon_k - \epsilon_0$. Thus, it is recognized that the secondary electron intensity $N_0(E_k)$ emitted from the surface by ion neutralization should decrease with increasing Φ . For electron incidence, the surface barrier, i.e., the Fermi energy and the work function,^{5,6} prevents only the low-energy part of secondary electrons from leaving the solid. The essential difference between electron and ion bombardment is attributed to a large contribution of bulk electron density processes for electron impact, while surface processes are important for ion impact.

In conclusion, we found that the dependence of δ on Φ is opposite between electron and ion bombardment from the simultaneous measurements of δ with Φ for 30 species of metals. The reason why the δ dependency on Φ is opposite between electron and ion impact is not yet clear, but the different behaviors of secondary electron emission have been discussed on the basis of kinetic and potential emission and seem to be caused by different contributions of bulk and surface local electron densities through the excitation process of secondaries.

¹Y. Sakai, T. Yamada, T. Suzuki, T. Sato, H. Itoh, and T. Ichinokawa, *Appl. Phys. Lett.* **73**, 611 (1998).

²J. Dekker, *Solid State Physics* (Prentice-Hall, Englewood Cliffs, NJ, 1957), Chap. 17.

³H. Seiler, in *Electron Beam Interactions with Solid*, edited by D. F. Kyser, H. Niedrig, D. E. Newbury, and R. Shimizu (SEM, Chicago, IL, 1982), pp. 33–42.

⁴M. Rosler and W. Brauer, *Phys. Status Solidi B* **104**, 161 (1981).

⁵J. Schou, *Scanning Microsc.* **2**, 607 (1988).

⁶D. Hasselkamp, *Particle Induced Emission II* (Springer, Berlin, 1992), pp. 1–95.

⁷R. A. Baragiola, E. V. Alonso, and A. Oliva Florio, *Phys. Rev. B* **19**, 121 (1979).

⁸*Ion Implantation, Sputtering and Their Applications*, edited by P. D. Townsend, C. Kelly, and N. E. W. Hartly (Academic, London, 1976), Chap. 2.

⁹H. B. Michaelson, *J. Appl. Phys.* **48**, 4729 (1977).

¹⁰S. Hippler, D. Hasselkamp, and A. Scharmann, *Nucl. Instrum. Methods Phys. Res. B* **34**, 516 (1988).

¹¹E. J. Sternglass, *Phys. Rev.* **108**, 1 (1957).

¹²E. M. Baroody, *Phys. Rev.* **78**, 780 (1950).

¹³C. J. Tung, J. C. Ashley, and R. H. Ritchie, *Surf. Sci.* **81**, 427 (1979).

¹⁴J. Schaefer and J. Hoelzl, *Thin Solid Films* **13**, 81 (1972).

¹⁵N. D. Lang and W. Kohn, *Phys. Rev. B* **1**, 4555 (1970); **3**, 1215 (1971).

¹⁶H. D. Hagstrum, in *Electron and Ion Spectroscopy of Solids*, edited by L. Fiermans, J. Vennik, and D. Dekeyser (Plenum, New York, 1978).

¹⁷H. D. Hagstrum, *Phys. Rev.* **89**, 244 (1953).